

Incorporation of Metal Nanoparticles into a Double Gyroid Network Texture

Masayuki Adachi,[†] Arimichi Okumura,[†] Easan Sivaniah,^{†,§} and Takeji Hashimoto^{*,†,‡,⊥}

Department of Polymer Chemistry, Graduate School of Engineering, Kyoto University, Katsura, Kyoto 615-8510, Japan, and Advanced Science Research Center, Japan Atomic Energy Agency, Ibaraki Pref. 319-1195, Japan

Received May 17, 2006; Revised Manuscript Received July 23, 2006

ABSTRACT: Palladium nanoparticles have been successfully incorporated into a porous diblock copolymer template using a novel technique. An ordered bicontinuous double gyroid phase was created from poly(isoprene)-*block*-poly(2-vinylpyridine). The poly(isoprene) matrix of this structure was subsequently removed by ozonolysis, creating a high specific surface area material composed of a poly(2-vinylpyridine) double gyroid network texture. Palladium ions were then adsorbed and reduced within the material. Large loadings of the nanoparticles were possible. It was also possible to kinetically control the dimensions (~5–10 nm) and number density of the nanoparticles. Because of the high porosity and specific surface area of the template, this technique is very promising for high-performance catalysts and other applications.

Introduction

There has been a lot of recent interest in the preparation of metal nanoparticles incorporated within a polymer matrix. And for good reason since such materials hold great potential in several existing technologies and sciences. Ciebiën et al. provide a good review of some of these uses.¹ A more recent review by Ulbricht looks specifically at a subset of applications in membrane and catalyst technology.² For example, the catalytic activity of palladium (Pd) and platinum particles in heterogeneous hydrogenation reactions is strongly dependent upon their total specific surface area, particle dimension, and the nature of the interaction between the matrix components.^{3,4} As another example, Pd is theorized to have ferromagnetic properties when the particles sizes are small enough for quantum size effects to be relevant and when the dimensions of the particles are strongly asymmetric.^{5–8} The polymer matrix, on the other hand, can have a range of properties, e.g., hydrophobicity and heat and chemical resistance; moreover, they are typically cheap and easily processable.

Polymer/Pd particle composites, a polymer matrix containing Pd particles with an average diameter of ~nm, have been prepared by several different methods in the past: by the condensation of metal vapors into a solvent containing monomer that is subsequently polymerized⁹ or by the chemical synthesis of polymers and copolymers with organometallic moieties that are subsequently reduced to Pd atoms.¹⁰ Another form of Pd particle preparation initiated by Hirai et al. was the reduction of Pd ions in aqueous solution in the presence of a polyelectrolyte, thereby stabilizing the Pd atoms against large-scale flocculation by both steric and double-layer interactions.¹¹ Horiuchi and co-workers have worked extensively on the thermal and e-beam reduction of palladium–acetyl acetonate precursors in polymer matrices.^{12,13}

In our previous work we have used a reduction technique within nonaqueous solutions containing hydrophobic homopolymers and copolymers. The solutions were subsequently solvent cast to produce the polymer/Pd particle composites with Pd particles of an average diameter of ~5 nm. The use of a diblock copolymer made it possible to promote the selective incorporation of the Pd particles within one of the microphases.¹⁴ This phenomenon arose from the preferential interactions of the Pd particle with one copolymer species over the other. This type of behavior was studied in depth in our group by varying the length of the block copolymers and by performing the reduction process in different order, i.e., mixing prereduced particles with the polymer within solution^{14,15} or performing the reduction of Pd²⁺ ions in microdomain spaces developed by microphase separation in block copolymer solutions.¹⁶ In this manner we have demonstrated several methods for producing well-defined Pd particle sizes within the polymer matrix. Such reports fit well with contemporary research by other research groups on the incorporation of metallic and semiconducting nanoparticles into block copolymer matrices.^{17–19}

In our most recent research we have been interested in producing porous polymer membranes loaded with the Pd nanoparticles. We believe such a material is advantageous in several applications because of the better access to reactive sites within the polymer matrix. The double gyroid (*Ia3d*) polymer microdomain structure is a very suitable candidate for such a bicontinuous structure and has been observed in diblock and triblock copolymer systems,^{20,21} through the combination of homopolymers and diblock copolymer systems²² or even through the combination of diblock copolymer systems.²³ The double gyroid structure also has superior mechanical properties than the more classical microphase structures, e.g., spherical and lamellar, arising from the fact that it is essentially two mirrored interleaved network structures.^{24,25} This type of structure has been exploited to create porous and relief ceramic structures by selectively degrading one part of the polymer and oxidizing the silicon-containing portion.²⁶

In this work we will demonstrate a different processing technique to produce a porous cross-linked double gyroid texture that can be loaded with Pd particles. In doing so, we show that

* Corresponding author.

[†] Kyoto University.

[‡] Japan Atomic Energy Agency.

[§] Present address: Department of Chemical Engineering, Texas Tech University, Lubbock, TX 79409.

[⊥] Present address: Advanced Science Research Center, Japan Atomic Energy Agency, Tokai-mura, Naka-gun, Ibaraki Pref. 319-1195, Japan.

it is possible to kinetically control the dimensions of the Pd particles.

Experimental Method

The poly(isoprene) (PI) homopolymer and poly(isoprene)-*block*-poly(2-vinylpyridine) (PI-*b*-P2VP) diblock copolymer used in this work were synthesized by living anionic polymerization, as described elsewhere.²⁷ The PI and poly(2-vinylpyridine) (P2VP) component of the diblock had a number-averaged molecular weight, M_n , of 2.58×10^4 and 4.05×10^4 and a polydispersity index, M_w/M_n , of 1.04. The PI homopolymers had a number-averaged molecular weight, M_n , of 3.84×10^3 and a M_w/M_n of 1.06.

To create the gyroid microphase texture, PI and PI-*b*-P2VP were weighed together into a chloroform solvent so that the weight fraction of P2VP in the polymer mixture was 0.34. The homogeneous solution (5 wt % of the polymer mixture in solvent) was allowed to evaporate slowly over a period of a month. The resulting solution cast polymer film was dried in a vacuum oven for 2 days at 80 °C to remove the final traces of solvent. The final dimensions of such polymer films were typically 0.5 mm thick disks with a 20 mm radii.

Pieces of the cast film was exposed to diiodobutane (DIB) vapor at 80 °C for up to 2 days to selectively cross-link the P2VP network microphases.²⁸ DIB is also a preferential stain for the P2VP phase for use with transmission electron microscopy (TEM). The samples were then dried under vacuum to remove unreacted DIB. It was possible to alter the degree of cross-linking by varying the exposure time. The degree of cross-linking (DC) was defined as the number of DIB units absorbed and reacted divided by the total number of pyridine pairs present within the sample. Thus, DC can be determined from a knowledge of chemical composition of the polymer mixture and the weights of the samples before and after exposure. After long exposures DC was found to be 0.85 ± 0.05 . In the finite exposure times used in this study, 6, 12, and 24 h, DC was found to be 0.24, 0.27, and 0.55, respectively.

The PI matrix of the polymer was then degraded by ozonolysis in an O₃/heptane solution for 48 h. The degraded PI phase was subsequently removed by immersion in a hexane/trimethyl phosphonate solution for 24 h. A more detailed analysis of the consequences of the above techniques in creating the double gyroid porous texture was described elsewhere.²⁸

The post-degraded P2VP network was then soaked in a warm bath (80 °C) made from a 50 mL (25:75) mixture of 1-propanol and toluene. This mixed solvent contained 0.3 g of palladium acetylacetonate [Pd(acac)₂], which has been shown to be reduced by 1-propanol to palladium atoms.¹⁴ The amount of Pd(acac)₂ added to the solvents was intended to give an initial ion concentration in excess to the total number of pyridine units in the system. It is expected that this reduction process will occur within the polymer network but also can occur within the solution itself. The immersion time was controlled and varied from 1 h to 4 days as part of the experimental strategy. Additionally, the toluene was replaced with other solvents—benzene, 1,4-dioxane, and acetone—in order to investigate this influence upon Pd nanoparticle growth. A schematic depicting the preparation process of the Pd filled polymer system is summarized in Figure 1.

The microdomain structure of the samples prepared in this way were then examined by TEM (JEM2000FXZ, JEOL, Tokyo, Japan) operated at 120 kV. Ultrathin sections for TEM were obtained using a Reichert-Nissei Ultracut-S cryo-ultramicrotome. The size distribution of the Pd nanoparticles observed in the resulting micrographs was then analyzed by use of standard imaging software. This approach was endorsed by independent manual measurements on selected micrographs. Typically 300–400 particles were counted and measured within a 0.16 μm² area of the micrograph. Since the sampled area of the micrographs was constant, the number of particles found represents the particle number density, N .

Results and Discussion

The microdomain structure of the double gyroid phase is itself an interesting and complex issue. While it is outside the scope

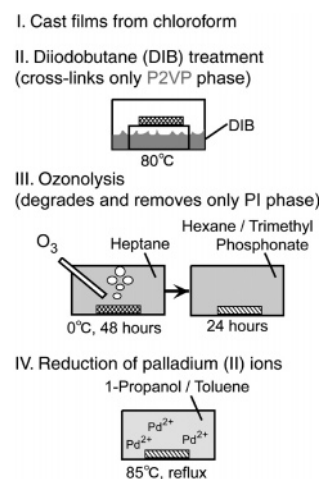


Figure 1. Schematic of the process for preparation of the Pd-loaded double gyroid textures.

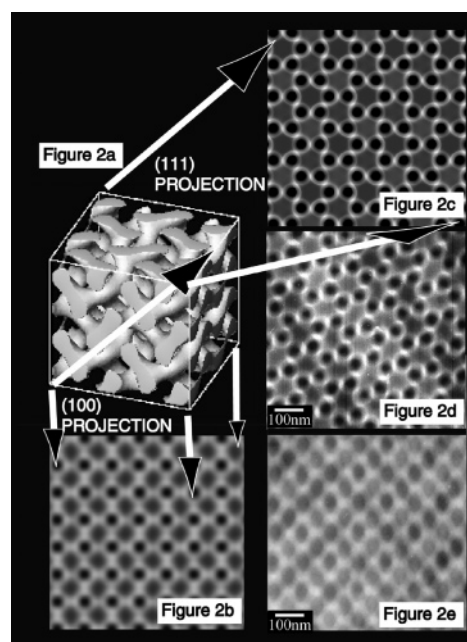


Figure 2. (a) 3-D rendering of double gyroid unit cell. Slices of the unit cell along the (100) and (111) crystal plane are shown in (b) and (c), respectively. The brightest and darkest regions refer to areas of the TEMS slice where there is a predominant amount of PI and P2VP, respectively. Parts e and d respectively show two TEM micrographs, which are similar to (b) and (c), of the P2VP-*b*-PI/PI blend after cross-linking but no further processing. The bright regions refer to the PI domain. The dark regions refer to the DIB-stained P2VP phase.

of discussions of the current paper, it is worthwhile to show representative TEM micrographs of the as-cast PI-*b*-P2VP/PI microdomain after staining with DIB but without any further processing and without the addition of Pd particles (Figure 2). The computer graphic shown in Figure 2a depicts a 3D unit cell structure of the double gyroid single crystal, constructed on the basis of an equation in differential geometry that has the $Ia\bar{3}d$ space group symmetry. Slices (of thickness equal to the unit cell repeat length) of this structure are taken parallel to the (100) and (111) plane. The overall contrast of the slices is obtained by integrating the local contrast of the domains along the direction normal to the slice. The local contrast was given according to a pseudo-electron scattering density proportional to the contributions of the degraded PI (density assigned as 0) and DIB-stained P2VP domains (density assigned as 1), both of which are present at a given position in the slice. In this

way, we produce a TEM simulation (TEMS),²⁹ numerically calculated TEM images for slices with a given thickness and direction of the model structure, to compare to the TEM images actually observed. This is shown very clearly by comparing parts c and d of Figure 2 which show respectively the TEMS for the slice parallel to the (111) plane viewed along the [111] direction and an actual TEM from an ultrathin section of PI-*b*-P2VP/PI blend. This comparison was also seen between a TEMS slice parallel to the (100) plane viewed along the [100] direction and experiment (parts b and e of Figure 2, respectively). More details of this computer simulation method can be found elsewhere,²⁹ though there are also independently existing software that use similar generation methods, e.g., TEMsim.^{30,31}

TEM micrographs of the polymer system *after* cross-linking and degradation have indicated that this microdomain structure remains, and subsequent figures in this paper contain an underlying image similar to Figure 2e. Hence, the removal of the PI matrix phase does not affect the skeletal structure of the P2VP double gyroid network. It is assumed that the primary reason for a lack of collapse of the double networks, which interpenetrate each other without touching, after PI removal is due to a grain boundary structure that acts as a scaffold for the P2VP double gyroid network.

Figure 3 shows representative TEM of the polymer structure after reduction in a 1-propanol/toluene/ Pd(acac)₂ bath for a range of times. The Pd particles, approximately spherical in shape, are visibly growing in size with the reduction time. Moreover, in the final stages of the time scale shown in Figure 3 the particle number density, N , is decreasing. It also *seems* that the Pd particles are to be found in the P2VP phase (stained dark by DIB) and not in the void areas. That this is not immediately apparent is a testament to the three-dimensional nature of the double gyroid texture. Pd particle that may seem (from the micrographs) to be within the void phase (bright phase) of the micrographs are more likely to be found at a lower or upper overlapping layer of the P2VP gyroid network in the ultrathin section used for the TEM observation. However, it is unequivocally proved that the particles reside only in the P2VP phase by conducting similar experiments within a lamellar microphase morphology. Figure 4 shows just such a micrograph, where the processing described above has been applied to the pure PI-*b*-P2VP polymer forming a lamellar morphology and the degraded structure has been immersed in the Pd(acac)₂ bath for 48 h. It should be noted that the P2VP lamellae (stained dark) and the degraded PI lamellae (existing as a void space) are oriented with their interfaces parallel to the electron beam so that two sets of lamellae are not overlapping.

TEM micrographs of the double gyroid polymer samples, subject to the reducing reaction in the Pd bath, were collected in order to obtain a quantitative measure of the nature of the particle growth mechanism. Particle analysis software allowed us to determine the population and size distribution as a function of time. Illustrative examples of the particle size distribution are shown in Figure 5. It is notable that the initial size distribution is quite narrow and broadens at longer times. The distributions clearly reinforce the information gleaned from the TEM. Fitting the distributions with a normal Gaussian model, we can extract the dynamics of the mean particle diameter, \bar{D} (Figure 6). The half-width at half-maximum (hwhm) normalized by \bar{D} is roughly equivalent for the three data sets shown in Figure 5, i.e., 0.20, 0.20, and 0.17 for the particle size distributions after 1, 13, and 120 h, respectively.

There is a clear power law dependence for \bar{D} which goes as $t^{1/6}$ (Figure 6a). At the same time we see that the number density,

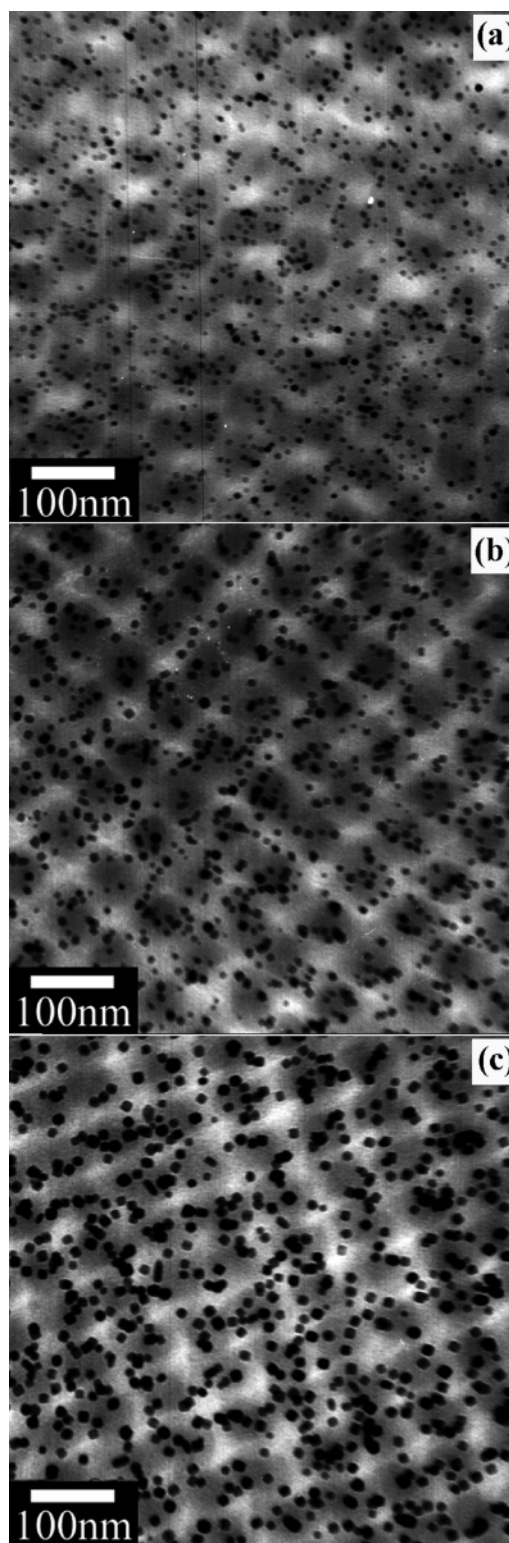


Figure 3. TEM micrographs of Pd-loaded gyroid network after reduction in 1-propanol/toluene/Pd(acac)₂ for different times at 85 °C: (a) 13, (b) 24, and (c) 48 h. The bright regions refer to the degraded PI domain (void spaces). The dark regions refer to the DIB stained P2VP phase. The darkest spots are the Pd clusters.

N , of particles appears to first rise quickly as a function of time before decaying to reach a constant value of about 280 particles per 0.16 μm^2 (Figure 6b). It is worthwhile to consider the various possible processes that are at work during immersion of the polymer within the reducing bath. Both inside and outside of the swollen gyroid network, Pd²⁺ ions are being reduced to Pd atoms, and these atoms are subsequently aggregating into larger

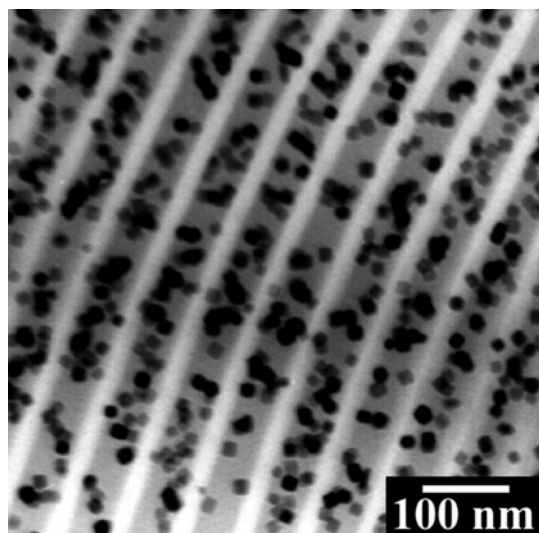


Figure 4. TEM micrograph of Pd loaded into a lamellar microphase. The bright regions refer to the degraded PI domains. The dark regions refer to the DIB-stained P2VP. The darkest spots are the Pd clusters.

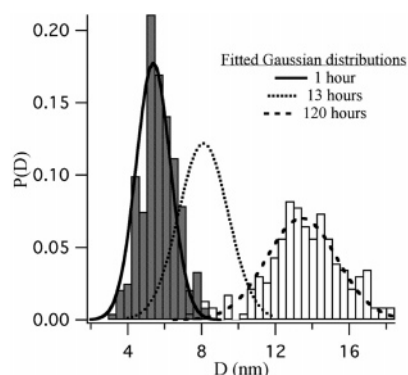


Figure 5. Particle size distributions and Gaussian fits from TEM micrographs of Pd particles reduced within the double gyroid texture in 1-propanol/toluene/ $\text{Pd}(\text{acac})_2$ for different reduction times at 85 °C. The y-axis refers to the normalized probability density function $P(D)$, where $\int P(D) dD = 1$. Three different times are shown: 1, 13, and 120 h. The histogram for $t = 13$ h has been omitted for clarity.

particles. The number of these particles that make their way into the swollen P2VP polymer network will be a complex function of several parameters that depend on the relative interaction between the Pd^{2+} ions and the Pd atoms with the solvent and with the P2VP network. The picture is slightly simpler if we consider only Pd^{2+} ions that have diffused and adsorbed into the P2VP texture. This process is shown schematically in Figure 7. The adsorbed ions will be reduced to Pd atoms in the presence of 1-propanol in the swollen cross-linked network. These atoms quickly aggregate to small Pd atom clusters or particles (process 1). There may be an exchange of ions between the inside and the outside of the network driven by osmotic pressure (process 2). The number of Pd particles will increase with time as a consequence of the reduction and aggregation. These particles will then coalesce within the texture into larger particles (processes 3a and 3b). As a consequence, the particle number tends to decrease with time. However, the precise nature of this latter stage is subject to speculation.

There are two feasible dominant modes of particle growth. The first, often known as Ostwald ripening and predicted by a Lifschitz–Slyozov–Wagner (LSW) model,^{32,33} might occur by an evaporation/condensation mechanism of small Pd clusters existing in the neighborhood of large Pd clusters whereby Pd atoms from a smaller particle aggregate evaporate into the matrix

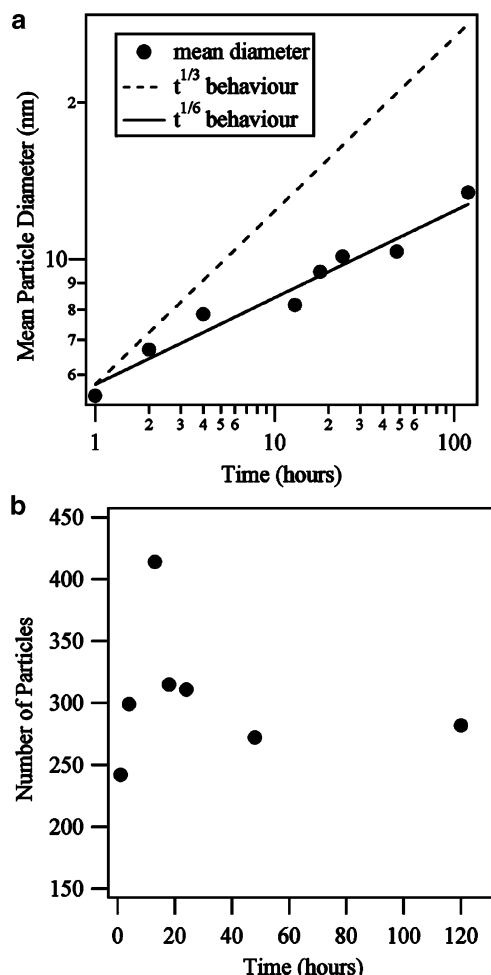


Figure 6. (a) Experimental \bar{D} vs time for the Pd reduction in 1-propanol/toluene/ $\text{Pd}(\text{acac})_2$ at 85 °C extracted from particle analysis (full circles). Also shown are the power law predictions from the diffusion and coalescence model (without hydrodynamic interactions), full line, and the LSW theory, dashed line. (b) The number of particles in a $0.16 \mu\text{m}^2$ area of the TEM micrograph as a function of time.

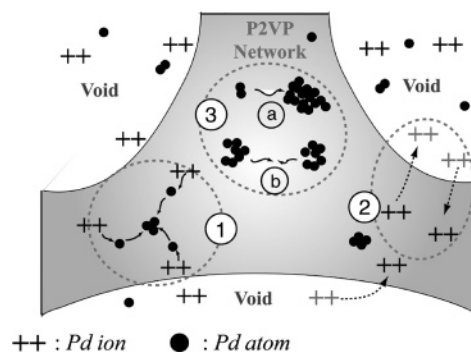


Figure 7. Schematic of the various processes that will occur during the immersion of the gyroid network into the Pd reducing bath. The three processes highlighted are discussed in the text.

(the P2VP network) and diffuse toward a larger aggregate (process 3a), driven by the Gibbs–Thomson effect. The alternative model would be that of diffusion of the aggregates within the matrix and the subsequent formation of a larger aggregate by coalescence (process 3b). Both models are characterized by a power law time dependence for \bar{D} , as t^n . The LSW model predicts an exponent of $1/3$. The diffusion and coalescence model has $n = 1/6$ and $1/3$, respectively, in the absence and presence of hydrodynamic interactions.³⁴ These predictions are plotted in Figure 6a, and it is clear that the

diffusion and coalescence model without hydrodynamic interactions has a very good agreement.

The coarsening process of metal particles via either of the two models mentioned were originally proposed to occur in hot melts of binary metal alloys, e.g. Oki et al.³⁵ Whether or not such coarsening occurs in the swollen polymer network at low temperatures is not self-evident. There are other caveats to using the coarsening models since the exponents are based on theory where the total number of Pd atoms is conserved during the coarsening process. Since there is a bath of Pd^{2+} ions surrounding the network, and Pd^{2+} ions can constantly be fed into the network via diffusion driven by osmotic pressure of ions as a consequence of reduction and annihilation of Pd^{2+} ions within the network phase, this will not necessarily be the case. However, we might argue that there is a critical concentration of Pd^{2+} ions that may be adsorbed into the P2VP texture and reduced into Pd atoms. We can argue that there is a given concentration of Pd^{2+} ions inside and outside of the P2VP network immediately before the reduction of Pd^{2+} ions starts to occur. There may be an exchange or interdiffusion of ions between inside and outside of the networks during the reduction, but the total ion concentration subject to reduction will not be altered by the exchange of ions. The reduction of Pd^{2+} ions inside and outside the network are effectively independent of each other, and the reduced atoms effectively stay in the same region, i.e., either within the network or outside of it. In this way a quasi-conserved system might exist. Such a notion is corroborated by the behavior of N as a function of time. The initially fast increase in particle number density, N , could refer to the reduction of Pd ions to atoms and the aggregation of atoms into particles, as shown by process 1 in Figure 7. The subsequent slower decay of N suggests that the large number of small Pd particles thus created grow into a smaller number of larger Pd particles via process 3a or process 3b. However, experiments to verify this are currently underway. It is prudent at this stage to only show that we can control the size and distribution of Pd particles dynamically. Such control will be critical in the potential application of such materials.

There are other factors that can influence the nature of Pd particle growth in the matrix. One is the degree of cross-linking achieved with DIB. Cross-linking density alters the degree to which the network can swell with the 1-propanol/toluene/ $\text{Pd}(\text{acac})_2$ solution and so may affect the mobility of the Pd atoms and particles. However, it was found that there was no discernible change in particle size for samples exposed in the reducing bath for the same amount of time but which had previously been exposed to DIB vapor for differing times (6, 12, and 24 h). As explained within the previous section, we were able to quantify the extent to which the sample had been cross-linked using the parameter DC, but this measure gives us no clue as to the mesh size of the cross-linked network. This latter parameter is probably the most useful way to characterize the mobility of the Pd particles in the network, and dynamic mechanical experiments are underway currently to extract this parameter.

Another influence on particle growth is the nature of cosolvent that is used with 1-propanol. A variety of other solvents were tried, and this effect is shown graphically in Figure 8. It is apparent that the particle size for a given reduction time (18 h) and temperature (85 °C) can be altered with the type of solvent used. Both benzene (Figure 8a) and 1,4-dioxane (Figure 8b) produce larger Pd aggregates than when toluene (Figure 6a) is used. Acetone (Figure 8c), on the other hand, produced significantly smaller Pd aggregates. This conjecture is compli-

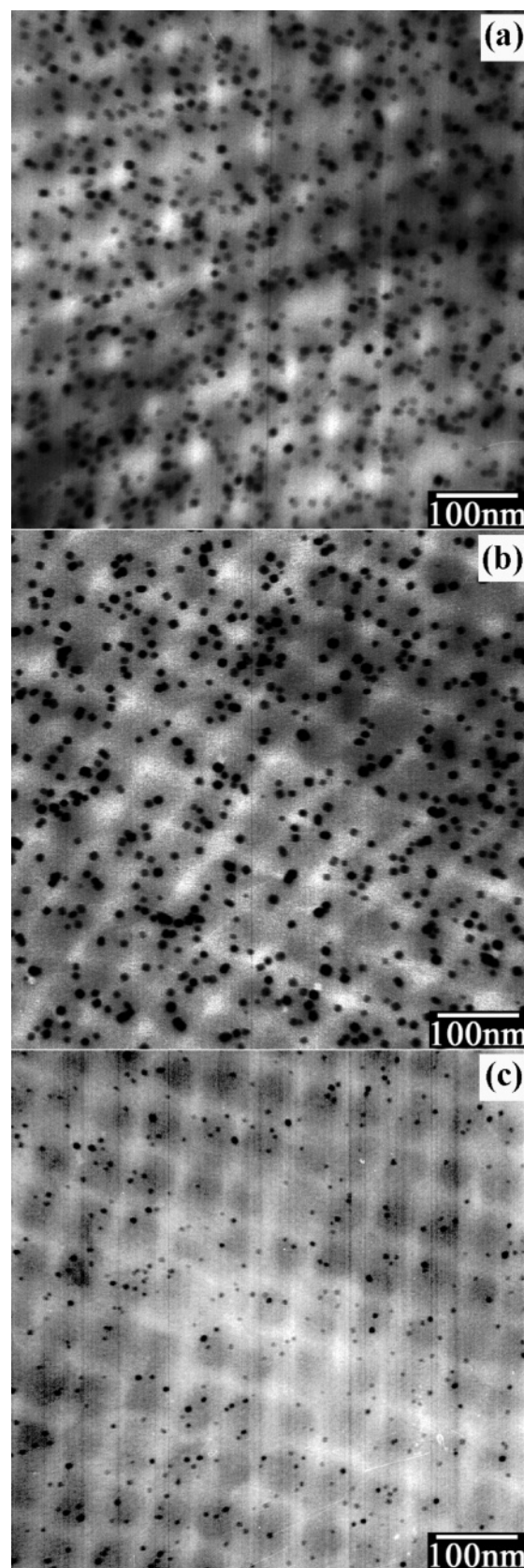


Figure 8. Comparison of the particle sizes produced in P2VP networks immersed (for 18 h) into Pd reducing baths that have different cosolvents with 1-propanol. The cosolvents are (a) benzene, (b) 1,4-dioxane, and (c) acetone. The reducing temperature is 85 °C for (a) and (b) and 55 °C for (c).

cated by the fact that the 1-propanol/acetone/ $\text{Pd}(\text{acac})_2$ bath was operated at 55 °C due to the lower boiling point of acetone. However, this does show that the three-way nature of interac-

tions between Pd²⁺, the cosolvent, and the polymer matrix is a factor in the reduction and aggregation process.

Conclusions

The use of voiding or porogens and subsequent backfilling with nanoparticles as a general technique to introduce hybrid character to materials is widespread. We believe that the work we have shown represents a novel method for achieving high loadings of metal particles into a polymer texture. The open structure afforded by the voided bicontinuous gyroid architecture forms the in situ ambience, swollen by an organic solution, within which metal ions are reduced. The high degree of loading is partly a result of reduction conditions within an organic solvent. Metal ions in an aqueous solvent would have difficulty to sufficiently swell the voided P2VP texture. We would like to note also the possibility that the metal ions in an aqueous solution mixed with a proper amount of an organic solvent may enable us to localize the reduced metal ions selectively near the surface of the texture.

The technique has several other qualities that make it attractive from an application point of view. We can produce Pd aggregates in a very controllable fashion with well-defined size distributions within well-controlled ordered textures having nanoporosity. The double gyroid network texture upon which we impose the particles is a highly interconnected porous network. Cross-linking of the texture makes it more stable to chemical and physical attack. The high porosity also implies a high specific surface area which is often a sought-after quality in catalyst technology. However, the general technique is also one that might be applied in other fields such as tunable dielectric material for optical processing. One concern might be the mechanical integrity of the system. As mentioned, we believe that the double gyroid network does not collapse due to the support of the grain boundary structure, but such systems tend to be fragile.

Moreover, the work involves some interesting phenomena and poses a fundamental question regarding the nature of metal particle aggregation and growth within swollen polymer networks inside the gyroid textures. The entire question of metal nanoparticle aggregation in polymer systems is not one that has been dealt with so far in any detail. However, there are interesting analogies to the behavior observed in binary metal systems where LSW or diffusion-coalescence type behavior is predominant. We would like to know whether our apparent diffusion and coalescence behavior is something that arises from the nonconservative nature of our system or whether it arises from the nature of the polymer microdomain structure or from another effect. It is not possible to conjecture further on this without having some data concerning simpler systems, e.g., the metal particle growth in homopolymers matrices containing the metal ions and reducing agents, and this is a current topic of research.

We should note that the above argument is related to the following fundamental scientific problems, the clarification of which deserves future study. The state of Pd atoms changes from a gaseous to a liquid state and eventually to a solid state. A gaseous state is relevant to isolated Pd atoms themselves or to a very small Pd clusters. A liquid state occurs during the growth of clusters via processes 3a and 3b or via the absorption of gaseous Pd atoms at the surfaces of the clusters. The growth of the clusters via processes 3a and 3b would be pinned when the clusters are solidified. Wide-angle X-ray diffraction studies after completion of the reduction reaction revealed that the nanoparticles exhibit diffraction peaks at the same Bragg angles as those for bulk Pd metals.

A more detailed analysis of the application potentials for the resulting hybrid catalyst material is left for future research. There are some outstanding questions that have arisen from this research. For example, the exact location of the palladium nanoparticles—are they located within the gyroid texture or at its surface—will have implications for the catalytic efficiency of the materials. Such questions are answered through either more involved ET-TEM studies,³⁶ small-angle X-ray scattering (SAXS),³⁷ or more direct studies of Pd-catalyzed reactions.

References and Notes

- (1) Ciebiën, J. F.; Clay, R. T.; Sohn, B. H.; Cohen, R. E. *New J. Chem.* **1998**, 22, 685.
- (2) Ulbricht, M. *Polymer* **2006**, 47, 2217.
- (3) Mayer, A. B. R.; Mark, J. E. *J. Polym. Sci., Part A: Polym. Chem.* **1997**, 35, 3151.
- (4) Berkovich, Y.; Garti, N. *Colloids Surf., A* **1997**, 128, 91.
- (5) Esumi, K.; Wakabayashi, M.; Torigoe, K. *Colloids Surf., A* **1996**, 109, 55.
- (6) Mendoza, J.; Morales, F.; Escudero, R.; Walter, J. *J. Phys.: Condens. Matter* **1999**, 11, L317.
- (7) Nunomura, N.; Teranishi, T.; Miyake, M.; Oki, A.; Yamada, S.; Toshima, N.; Hori, H. *J. Magn. Magn. Mater.* **1998**, 177–181, 947.
- (8) Teranishi, T.; Hori, H.; Miyake, M. *J. Phys. Chem. B* **1997**, 101, 5774.
- (9) El-Shall, M. S.; Slack, W. *Macromolecules* **1995**, 28, 8456.
- (10) Ciebiën, J. F.; Cohen, R. E.; Duran, A. *Supramol. Sci.* **1998**, 5, 31.
- (11) Hirai, H.; Nakao, Y.; Toshima, N. *J. Macromol. Sci., Chem.* **1979**, A13, 727.
- (12) Horiuchi, S.; Fujita, T.; Hayakawa, T.; Nakao, Y. *Langmuir* **2003**, 19, 2963.
- (13) Yin, D.; Horiuchi, S.; Masuoka, T. *Chem. Mater.* **2005**, 17, 463.
- (14) Tsutsumi, K.; Funaki, Y.; Hirokawa, Y.; Hashimoto, T. *Langmuir* **1999**, 15, 5200.
- (15) Okumura, A.; Tsutsumi, K.; Hashimoto, T. *Polym. J.* **2000**, 32, 520.
- (16) Hashimoto, T.; Harada, M.; Sakamoto, N. *Macromolecules* **1999**, 32, 6867.
- (17) Bockstaller, M. R.; Thomas, E. L. *Phys. Rev. Lett.* **2004**, 93.
- (18) Chiu, J. J.; Kim, B. J.; Kramer, E. J.; Pine, D. J. *J. Am. Chem. Soc.* **2005**, 127, 5036.
- (19) Lin, Y.; Boker, A.; He, J. B.; Sill, K.; Xiang, H. Q.; Abetz, C.; Li, X. F.; Wang, J.; Emrick, T.; Long, S.; Wang, Q.; Balazs, A.; Russell, T. P. *Nature (London)* **2005**, 434, 55.
- (20) Avgeropoulos, A.; Dair, B. J.; Hadjichristidis, N.; Thomas, E. L. *Macromolecules* **1997**, 30, 5634.
- (21) Hajduk, D. A.; Harper, P. E.; Gruner, S. M.; Honeker, C. C.; Kim, G.; Thomas, E. L.; Fetters, L. J. *Macromolecules* **1994**, 27, 4063.
- (22) Winey, K.; Thomas, E. L.; Fetters, L. J. *Macromolecules* **1992**, 25, 422.
- (23) Spontak, R. J.; Fung, J. C.; Braunfeld, M. B.; Sedat, J. W.; Agard, D. A.; Kane, L.; Smith, S. D.; Satkowski, M. M.; Ashraf, A.; Hajduk, D. A.; Gruner, S. M. *Macromolecules* **1996**, 29, 4494.
- (24) Schick, M. *Physica A* **1998**, 251, 1.
- (25) Dair, B. J.; Honeker, C. C.; Alward, D. B.; Avgeropoulos, A.; Hadjichristidis, N.; Fetters, L. J.; Capel, M. C.; Thomas, E. L. *Macromolecules* **1999**, 32, 8145.
- (26) Chan, V. Z.-H.; Hoffman, J.; Lee, V. L.; Iatrou, H.; Avgeropoulos, A.; Hadjichristidis, N.; Miller, R. D.; Thomas, E. L. *Science* **1999**, 286, 1716.
- (27) Hashimoto, T.; Tsutsumi, K.; Funaki, Y. *Langmuir* **1997**, 13, 6869.
- (28) Okumura, A.; Nishikawa, Y.; Hashimoto, T. *Polymer*, in press.
- (29) Nishikawa, Y. Interface Curvatures of Bicontinuous Phase-structures in Two-component Polymeric Systems. Ph.D. Thesis, Kyoto University, Kyoto, 1999.
- (30) Hoffman, J. <http://www.msri.org/about/sgp/jim/software/temsim>.
- (31) Wohlgemuth, M.; Yufa, N.; Hoffman, J.; Thomas, E. L. *Macromolecules* **2001**, 34, 6083.
- (32) Wagner, C. Z. *Electrochem.* **1961**, 65.
- (33) Lifshitz, I. M.; Slyozov, V. V. *J. Phys. Chem. Solids* **1961**, 19, 35.
- (34) Gunton, J. D.; San Miguel, M.; Sahni, P. S.; Dynamics of First-Order Transitions. In *Phase Transitions and Critical Phenomena*; Domb, C., Lebowitz, J. L., Eds.; Academic Press: New York, 1983; Vol. 8.
- (35) Oki, K.; Sagana, H.; Eguchi, T. *J. Phys. C* **1977**, 7, 414.
- (36) Yamauchi, K.; Takahashi, K.; Hasegawa, H.; Iatrou, H.; Hadjichristidis, N.; Kaneko, T.; Nishikawa, Y.; Jinai, H.; Matsui, T.; Nishioka, H.; Shimizu, M.; Fukukawa, H. *Macromolecules* **2003**, 36, 6962.
- (37) Sakamoto, N.; Harada, M.; Hashimoto, T. *Macromolecules* **2006**, 39, 1116.